Experimental Study on the Mössbauer Effect of Fe in Several Iron Compounds

AUTHOR(S):

Nakamura, Takashi; Shimizu, Sakae

Experimental Study on the Mössbauer Effect of ^{57}Fe in Several Iron Compounds

Takashi NAKAMURA and Sakae SHIMIZU*

(Shimizu Laboratory)

Received August 11, 1964

The Mössbauer absorption spectra of some iron compounds have been observed using the 14.4 keV gamma-ray photons of ^{57}Fe. The quadrupole effect and isomer shift of $FeSO_4 \cdot 7H_2O$ have been measured. The internal magnetic field in Fe_2B has also been estimated. The effect of spin flopping at the Morin temperature has been confirmed for normal α-Fe_2O_3 (>1000Å). The absorption spectra of ultra-fine α-Fe_2O_3 particles (about 50Å and 150Å) have been observed at 120°K and 300°K, and no Morin transition has been found above at least 120°K with such ultra-fine particles. The spectrum of the particles of 50Å taken at 120°K showed six-line splitting, while at 300°K showed only two lines. This phenomenon may be explained by a motional narrowing due to the rapid relaxation of antiferromagnetic spins compared with the nuclear Larmor precession ($\sim 10^{-8}$ sec). The critical volume of particles and critical temperature for this transition have been found to be between 50Å and 150Å at 300°K and between 120°K and 300°K for particles of 50Å, respectively. It has also been found that for ultra-fine particles the recoilless fraction would decrease from that obtained with larger particles. Three iron oxyhydrate isomers, α-, β- and γ-FeOOH, were also used as absorbers and the following facts have been found: the Néel temperature for α-FeOOH may be close to 400°K and that for β-FeOOH may lie between 110°K and 300°K, while γ-FeOOH is paramagnetic above at least 110°K.

I. INTRODUCTION

When a free nucleus of mass M, decays from an excited state to the stable ground state by emission of gamma rays, it recoils with kinetic energy $R=E_0^2/2Mc^2$, where E_0 is the energy of the nuclear transition. Consequently, the emitted gamma-ray photon has an energy $E_\gamma=E_0-R$. As the necessary condition for the resonance absorption of the gamma rays in another nucleus of the same kind it is required to compensate for the recoil energy loss by, for example, high-speed rotation or thermal agitation. But, in the case where a nucleus is bounded tightly in a solid it cannot receive the recoil energy and the gamma-ray energy emitted is equal to the entire transition energy. This phenomenon is known as the recoilless resonance absorption and emission of gamma rays named "Mössbauer effect". This effect happened to be discovered by Mössbauer[1] in 1957 when he was investigating the nuclear resonance scattering of the 129-keV gamma rays from ^{191}Ir.

Later, the discovery of the Mössbauer effect in ^{57}Fe excited many workers' interests owing to its very large size; its persistence up to temperatures of

* 中村 尚司, 清 水 栄

over 1000°C and the very narrow line width. Especially, the extremely narrow line width provided possibilities, such as the measurement of the red shift of photons and the nuclear Zeeman effect, which were till then thought to be impossible. In the present day, various precise studies are being performed in the field of solid state physics.

We have recently performed a series of the Mössbauer measurements with some iron compounds in powder form using ^{57}Fe as a gamma-ray source, with an intention to obtain some information about their internal structure of solid state physical interest. In the present paper all aspects of our work are reported comprehensively.

In Chap. II a survey of the basic theory is treated and in the following chapter some details of the experimental apparatus are described. The iron compound samples examined by the present work are divided into four groups. As the first step of the work metallic iron and stainless steel foils have been used as the test materials in order to check the experimental apparatus and procedure to be adopted being satisfactory. The second group of materials studied are $FeSO_4 \cdot 7H_2O$, Fe_2B and normal (ordinary size) α-Fe_2O_3, for which we obtained some information on the internal magnetic field, isomer shift and quadrupole splitting.

On the magnetic properties of ultra-fine powders many researches have so far been published since the development of the theoretical studies by Frenkel and Dorfman[2], and Néel[3]. However, since only few studies on it by the method of the Mössbauer effect have been reported, in our work the Mössbauer spectra of very fine particles of α-Fe_2O_3 were observed. By such observations we could obtain some interesting information such as on the Morin transition and internal field in α-Fe_2O_3 itself and motional narrowing of fine particles.

As the fourth group of iron compounds to be studied we adopted three isomers of iron oxyhydrates, α-, β- and γ-FeOOH. On the internal structure of these three isomers some information has been obtained by the Mössbauer technique. The results obtained with these various iron compounds and some discussion are given in Chap. IV.

II. THEORY

II.1. Recoilless Fraction

Here the probability that the Mössbauer effect takes place, that is, the recoilless fraction will be treated. Now consider that the nucleus of an atom which is embedded in a solid emits or absorbs a gamma ray. The energy required for the nucleus to leave a lattice site is at least of the order of 10 eV. The recoil energy R, however, never exceeds a few tenths of an eV. Then, the nucleus cannot acquire translational energy. The energy that goes into motion of the entire solid is extremely small as neglected. The nuclear transition energy is thus shared between the gamma ray and the phonons (lattice vibrations). The Mössbauer transition occurs if the state of the lattice remains unchanged and the gamma ray gets the entire transition energy.

The state of the lattice can be specified by a set of quantum numbers $\{n_s\}$ expressing the lattice vibration. The probability $P(\{n_s{}^f\}, \{n_s{}^i\})$ describing the transition in which a gamma ray of momentum $\hbar\boldsymbol{K}$ is emitted by a nucleus whose center-of-mass coordinate is $\boldsymbol{X}_L$, while the lattice goes from a state specified by quantum numbers $\{n_s{}^i\}$ to a state specified by quantum numbers $\{n_s{}^f\}$ can be expressed by[4]

$$P(\{n_s{}^f\}, \{n_s{}^i\}) = |(\{n_s{}^f\}|\exp(i\boldsymbol{K}\cdot\boldsymbol{X}_L)|\{n_s{}^i\})|^2.$$

Therefore, the recoilless fraction is

$$P(\{n_s\}, \{n_s\}) = |(\{n_s\}|\exp(i\boldsymbol{K}\cdot\boldsymbol{X}_L)|\{n_s\})|^2. \tag{1}$$

Let us assume that the interatomic forces are harmonic. The result of the averaging is that each n_s can be replaced by its average value $\bar{n}_s$ at thermal equilibrium;

$$\bar{n}_s = 1/(e^{\hbar\omega_s/kT} - 1),$$

where ω_s is the frequency of the lattice vibration for the s-mode. And, moreover, we adopt the Debye model in which a density of lattice modes is proportional to $\omega_s{}^2$. Now, Eq. (1) becomes

$$P(\{n_s\}, \{n_s\}) = \exp\left\{-\frac{3E_0{}^2}{Mc^2k\Theta}\left[\frac{1}{4}+\left(\frac{T}{\Theta}\right)^2\int_0^{\Theta/T}\frac{xdx}{e^x-1}\right]\right\}. \tag{2}$$

From this result, it is found that when the recoil energy $R = E_0{}^2/2Mc^2$ is small, Debye temperature Θ is high and the ambient temperature T is low, the Mössbauer fraction is large.

II.2. Line Shape

The resonance absorption spectrum in the Mössbauer effect does not show the natural line width, but the broadening due to finite absorber thickness. Visscher[5] found that if emission and absorption lines have Lorentzian shapes of width Γ and no splitting, the overlap curve will be a Lorentzian but will show an apparent width Γ_{app} given by the following relations:

$$\left.\begin{aligned} &\Gamma_{app}/\Gamma = 2.00 + 0.27T, && 0 \leq T \lesssim 5; \\ &\Gamma_{app}/\Gamma = 2.02 + 0.29T - 0.005T^2, && 4 \lesssim T \lesssim 10. \end{aligned}\right\} \tag{3}$$

Here T is the effective absorber thickness and can be given by

$$T = f\,n\,a\,\sigma_0\,t, \tag{4}$$

where f is the fraction of gamma rays absorbed without energy loss given by Eq. (2), n the number of atoms per cubic centimeter, a the fractional abundance of the resonantly absorbing atoms, σ_0 the absorption cross section at resonance, and t the absorber thickness.

II.3. Isomer Shift

This effect arises from the shift of the nuclear energy levels due to the electrostatic interaction between the nuclear charge and the electronic charge within the nuclear volume. A shift can only be seen if the two nuclear states involved have different radii in two atomic systems which have different elec-

tronic wave functions at the nucleus of charge Ze. According to the calculation of surface charge model[6], the transition energy between two levels B and A becomes

$$E_0' = E_0 + \Delta E_B - \Delta E_A = E_0 + (2/3)\pi Ze^2|\psi(0)|^2[<R_A^2> - <R_B^2>].$$

Then, we find for the isomer shift between the emitter e and the absorber a,

$$\delta = E_a' - E_e' = (2/3)\pi Ze^2[<R_B^2> - <R_A^2>]\{|\psi(0)_a|^2 - |\psi(0)_e|^2\}, \qquad (5)$$

where $<R_A^2>$ and $<R_B^2>$ are the root-mean-square radii in the nuclear states A and B, respectively. $|\psi(0)_a|^2$ and $|\psi(0)_e|^2$ indicate the probability density of electrons at $r=0$, i. e., at the nucleus concerned in the absorber and emitter, respectively. Therefore, the shift δ provides the useful information on the effective radii of nuclei and the electronic states of solids.

II.4. Line Splitting

Extranuclear fields can remove degeneracy of nuclear levels by interacting with a nucleus, and split the absorption spectrum into components. These splittings caused by magnetic and electric hyperfine interactions are extremely important for the investigation of solid-state properties. Here two main interactions will be treated.

(i) **Magnetic dipole interaction.** The magnetic moment of the nucleus μ_I can interact with a magnetic field $\boldsymbol{H}$ which may be an externally applied field or a local effective field due to unpaired electrons in the atom and its neighbours. In the presence of the field the spatial degeneracy of the nuclear spin $\boldsymbol{I}$ is removed and each nuclear level splits into its $(2I+1)$ components. The energy shift of the sub-state m is then

$$\Delta E = -mg_I H, \qquad (6)$$

where g_I is the nuclear gyromagnetic ratio μ_I/I, and the direction of $\boldsymbol{H}$ has been taken as the axis of quantization O_z, and a separation between each sub-state level is

$$\Delta = \mu_I H/I. \qquad (7)$$

The ground-state spins and moments can be measured with conventional techniques, so that the magnetic moment of the excited state and the internal magnetic field can be both determined.

(ii) **Electric quadrupole interacton.** The nucleus has generally the electric quadrupole moment, due to its deformation from spherical symmetry. This moment can interact with the local electric field gradient. The Hamiltonian describing this quadrupole coupling $H = -\boldsymbol{Q}\cdot\nabla\boldsymbol{E}$ is derived, for example, by Abragam[7,8], where $\boldsymbol{Q}$ is the nuclear quadrupole moment and $\nabla\boldsymbol{E}$ the electric field gradient at the nuclear site. According to his result, when a crystal has an axis of symmetry, the sub-states are characterized by a definite $m(=I_z)$ value and the states of $\pm m$ are degenerate. The energy shifts are then given by

$$\varepsilon = \frac{e^2qQ}{4I(2I-1)}[3m^2 - I(I+1)], \qquad (8)$$

where $eq=\frac{\partial E_z}{\partial z}$.

Next the case of mixed magnetic dipole and electric quadrupole interactions will be discussed. On most occasions it is sufficient to consider the quadrupole coupling as a perturbation, since the effect is usually much smaller than the splitting produced by an internal effective magnetic field. Abragam[7,8] has given the first-order correction to the energies of the m states in the case of axially symmetrical crystal as

$$\varepsilon_m=\frac{e^2qQ}{8I(2I-1)}[3m^2-I(I+1)](3\cos^2\theta-1), \tag{9}$$

where θ is the angle between $\boldsymbol{Q}$ and $\nabla\boldsymbol{E}$.

III. EXPERIMENTAL APPARATUS

III.1. Source Preparation

In the present work the recoilless resonance emission and absorption have been observed using the 14.4-keV M1 transition line from the first excited level of ^{57}Fe formed by the electron capture decay of ^{57}Co; the decay scheme is shown in Fig. 1.

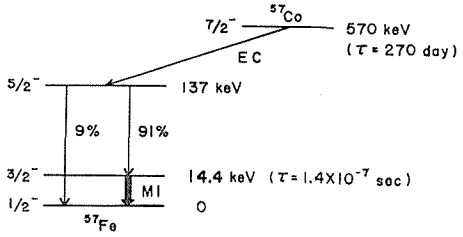

Fig. 1. Decay scheme of ^{57}Co.

The source was prepared by electroplating ^{57}Co in a carrier-free $^{57}CoCl_2$ solution onto a paradium plate, 0.1 mm thick and 15 mm in diameter, for about fifty hours. The ^{57}Co source co-plated with paradium was used from a reason that it gives the unsplit emission line being very sharp[9]. After plating, this source was annealed for two hours at about 850°C in a hydrogen atomosphere to diffuse ^{57}Co atoms uniformly into paradium plate. The activity of the source was estimated to be about 0.5 mC.

III.2. Absorber

In the present experiment ten kinds of the samples to be examined were used as the absorbers. Three of them were commercially available stainless steel foil, Fe powder and $FeSO_4\cdot 7H_2O$ powder. Powder of Fe_2B was prepared by melting a mixture of Fe and B powders at 1500°C. α-Fe_2O_3 was obtained by the calcination of α-FeOOH. Since it is known that when the calcination temperature becomes higher the particle size of α-Fe_2O_3 produced grows larger, we could obtain its powders of three different sizes by changing temperature for calcination; α-Fe_2O_3 of normal size (>1000Å), ultra fine particles with sizes of about 50Å and 150Å. The samples of α-, β- and γ-FeOOH were all prepared by

Professor T. Takada and his co-workers in our Institute. Details of the sample preparation of these isomers will be reported by them elsewhere.

The optimum thickness of all absorbers used was chosen to be about 10 mg /cm^2 of iron equivalent thickness, with the same number of iron atoms per cm^2, from a reason that, as understood from Eq. (3), when the absorber is very thin a quantity of the resonance absorption would be small and when very thick the resonance absorption spectrum would be broader. Throughout the work the absorber was placed just midway between the source and detector being mounted apart about 10 cm each other.

III.3. Measuring System

The experimental arrangement used in the present work is shown schematically in Fig. 2. The detection of the Mössbauer transmission is accomplished by measuring the intensity of the transmitted gamma rays as a function of the velocity with which the gamma-ray source is moved relative to the absorber. A relative velocity v with respect to the absorber produces a Doppler shift $(v/c)E_0$ in the gamma-ray emission line, where E_0 is the gamma-ray energy. The velocity v is defined as positive if the source moves toward the absorber.

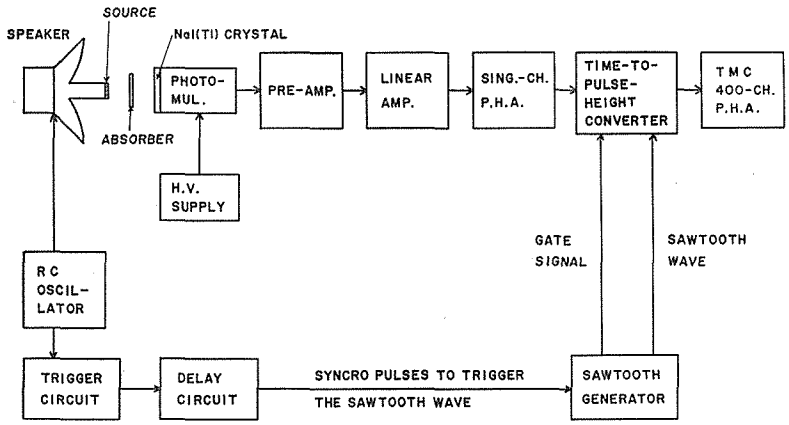

Fig. 2. Block diagram of the experimental arrangement.

The source was vibrated sinusoidally by mounting it on the top of a quartz pipe of about one cm in diameter cemented to the voice coil of a loudspeaker, which was driven sinusoidally at 30 cps, with a peak-to-peak amplitude of about one mm, by means of the RC oscillator device.

The transmitted gamma rays through the absorber were observed by a thin NaI(Tl) scintillator crystal, 0.5 mm thick and 25 mm in diameter, mounted on a Toshiba 7696 photomultiplier tube. The output pulses from this scintillation probe were fed to a single-channel pulse-height analyzer *via* a linear amplifier to select the 14.4-keV gamma ray. Since the long-term stability of the detector system was necessitated inevitably for the present measurement, it was checked at times during the course of the work by observing the scintillation spectrum of gamma rays from ^{57}Co.

On the other hand, the output pulses from the single-channel analyzer were modulated by the sawtooth waves in a time-to-pulse-height converter. The sawtooth waves were obtained by the bootstrap circuit and could be triggered only by the signals synchronized with the output frequency from the RC oscillator. By this device, pulse-height of the modulated outputs from the time-to-pulse-height converter could be proportional to the instantaneous source velocity at the time of emission of the corresponding gamma rays. The spectrum of modulated pulses can easily be observed by the use of a multi-channel pulse-height analyzer, for which we used a TMC 400-channel analyzer. The resonance spectrum was thus recorded as a function of the relative velocity between the source and absorber.

In the experiment using a voice coil of a speaker as the vibrator for the source, it is, in general, rather difficult to measure directly the instantaneous source velocity. In our work, six lines of metallic iron and a single line of stainless steel in the Mössbauer absorption spectra were observed in order to use positions of these lines as calibrations for the determination of the source velocity. For these the absolute velocities of the source have been exactly known from the results of other workers[10,11].

For measurements at liquid-nitrogen temperature the absorber was cooled using a cryostat as shown in Fig. 3. The temperature of the absorber was measured to an accuracy of $\pm 5°C$ by the use of a Cu-AuCo thermocouple screwed to the frame holding the absorber. To prevent water drops from dropping onto the source, the speaker was housed in a box made of styrofoam.

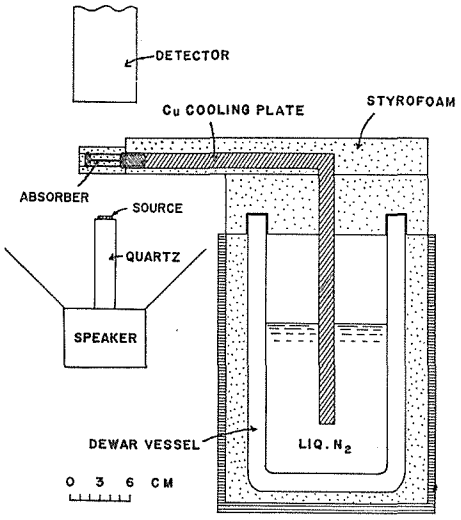

Fig. 3. Construction of the cryostat for cooling the absorber.

IV. APPLICATION TO SOME IRON COMPOUNDS: RESULTS AND DISCUSSIONS

IV.1. Metallic Iron

This ferromagnetic material has an internal magnetic field, so that the Zeeman effect will be expected and the nuclear levels involved may split into

components. The spins of the ground and first excited states of ^{57}Fe are 1/2 and 3/2, respectively. In the case where an unsplit source line and an unmagnetized absorber are used, the relative intensities of six absorption lines and the distances between them have been given theoretically[8,10], as shown in Fig. 4.

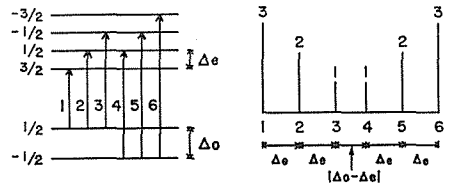

Fig. 4. Level diagram of ^{57}Fe. The numbers 1, 2, ……, 6 represent the peak positions from the left side of the Mössbauer absorption spectrum. The right-hand diagram gives the relative intensities of six absorption lines (shown as the numbers 1, 2, 3) and the spacings between them in the case with an unsplit source and an unmagnetized absorber.

The result of our observation is shown in Fig. 5. It is noted that the relative intensity ratio of these six lines we observed are 2.5 : 1.6 : 1.0 : 1.0 : 2.0 : 2.5, somewhat different from the theoretical value shown in Fig. 4. This discrepancy may be explained as being due to the background estimation and some characteristics of the detector system used. On this point no further study was performed, since the metallic iron absorber was adopted only with a purpose of using its six lines as calibrations for the source velocity, as described in the preceding chapter.

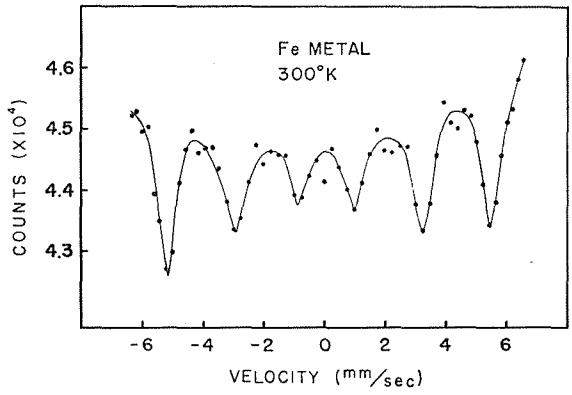

Fig. 5. Mössbauer absorption spectrum in a metallic iron absorber at 300°K.

IV.2. Stainless Steel

Stainless steel is a paramagnetic material having no internal magnetic field. It is also known to have a cubic lattice structure, in which the electric field gradient does not exist. The Mössbauer absorption spectrum is, therefore, very simple with only one peak. In Fig. 6 is shown the spectrum obtained. This line was also used as a calibration line for the source velocity.

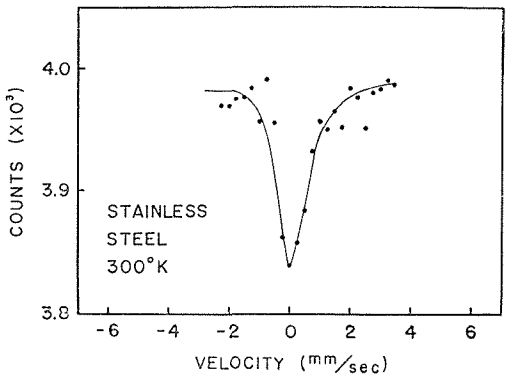

Fig. 6. Mössbauer absorption spectrum in a stainless steel absorber at 300°K.

IV.3. $FeSO_4 \cdot 7H_2O$

This iron compound is also paramagnetic and does not show the Zeeman splitting. However, a Fe^{2+} ion of $FeSO_4 \cdot 7H_2O$ has the $3d$ wave function of ^5D-state being lower symmetry, and the quadrupole effect should be expected. From Eq. (8) it is known that in the ground state $\varepsilon=0$ and the first excited level splits into following two components:

$$\left.\begin{aligned}\varepsilon(\pm 3/2) &= e^2qQ/4,\\ \varepsilon(\pm 1/2) &= -e^2qQ/4.\end{aligned}\right\} \qquad (10)$$

The levels of the absorber, the relative intensities of the absorption lines and distances between them are shown in Fig. 7.

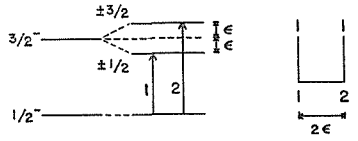

Fig. 7. Level diagram of ^{57}Fe bound in $FeSO_4 \cdot 7H_2O$. This diagram illustrates the electric quadrupole splitting. Right: the relative intensities of the absorption lines and the spacing between them in the case with an unsplit source and an unmagntized absorber.

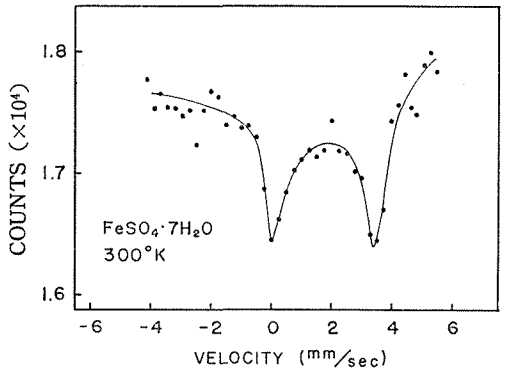

Fig. 8. Mössbauer absorption spectrum in $FeSO_4 \cdot 7H_2O$ at 300°K.

The observed spectrum showed two absorption lines as shown in Fig. 8. The intensity ratio of these two lines is about 1 : 1. The quadrupole shift ΔE and isomer shift δ obtained from the observed spectrum are

$$\Delta E = \varepsilon(\pm 3/2) - \varepsilon(\pm 1/2) = e^2qQ/2 = 3.26 \pm 0.1 \text{ mm/sec},$$
$$\delta = 1.67 \pm 0.1 \text{ mm/sec}.$$

These values obtained agree considerably with the other experimental values, $\Delta E = 3.20 \pm 0.05$ mm/sec and $\delta = 1.40 \pm 0.05$ mm/sec at room temperature, which have been reported by DeBenedetti *et al.*[12]. However, our value of δ larger by about 17% than that obtained by them may probably be due to the slight shift of the spectrum caused by the instability of the detector system or by fluctuation of the amplitude of vibration of the source during the measurement with this $FeSO_4 \cdot 7H_2O$ absorber.

IV.4. Fe_2B

This ferromagnetic material shows the line splitting and gives six lines as in the case with an metallic iron absorber. When no quadrupole effect exists, separations between the absorption lines 1 and 2, 2 and 3, 4 and 5, and 5 and 6 should be equal, as shown in Fig. 4. However, in this case, as shown in Fig. 9, values of these separations observed were not equal but 1.54 ± 0.13, 1.65 ± 0.16, 1.75 ± 0.10, and 1.71 ± 0.10 mm/sec, respectively. Taking account of the quadrupole effect, the level diagram of ^{57}Fe can be given as shown in Fig. 10. Since the spacings between the absorption lines 1 and 6, $S_{1,6}$, and 2 and 5,

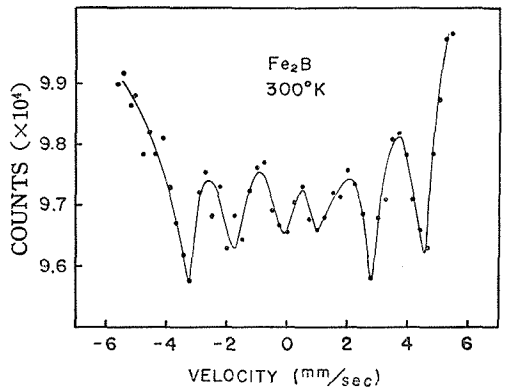

Fig. 9. Mössbauer absorption spectrum in Fe_2B at 300°K.

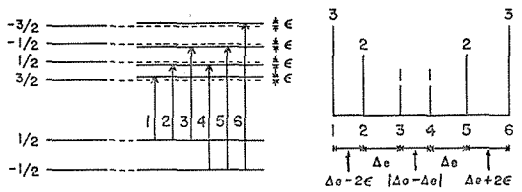

Fig. 10. Level diagram of ^{57}Fe when both the magnetic hyperfine splitting and the quadrupole interaction exist. Right: the relative intensities of the absorption lines and the spacings between them in the case with an unsplit source and an unmagnetized absorber.

$S_{2,5}$, are $|3\Delta_c-\Delta_0|$ and $|\Delta_c-\Delta_0|$, respectively, independent of the existence of the quadrupole effect, from Eq. (7) the following relation can be given:

$$\frac{S_{1,6}(Fe_2B)}{S_{1,6}(Fe)}=\frac{S_{2,5}(Fe_2B)}{S_{2,5}(Fe)}=\frac{H_i(Fe_2B)}{H_i(Fe)}. \tag{11}$$

Using this relation and our observations shown in Figs. 5 and 9 as well as adopting the value of the internal magnetic field at the iron nucleus as $H_i(Fe)=333\pm10$ kOe[10], $H_i(Fe_2B)$ could be determined as $H_i(Fe_2B)=245\pm15$ kOe.

Now, the differences between $S_{1,2}$ and $S_{5,6}$ can be given to be equal to 4ε, as shown in Fig. 10. From our measurement 4ε could be determined: $4\varepsilon=0.17$ mm/sec. As the present case involves the mixed interaction, for ^{57}Fe Eq. (9) becomes

$$\left.\begin{aligned}\varepsilon(\pm3/2)&=\frac{e^2qQ}{8}(3\cos^2\theta-1),\\ \varepsilon(\pm1/2)&=-\frac{e^2qQ}{8}(3\cos^2\theta-1).\end{aligned}\right\} \tag{12}$$

When $\theta=0°$, Eq. (12) will be Eq. (10) and $4\varepsilon=e^2qQ=0.17$ mm/sec.

When the quadrupole effect exists, the isomer shift δ can be expressed as $\delta=$(mid-point of $S_{1,6}$)$-\varepsilon=$(mid-point of $S_{2,5}$)$+\varepsilon$. By the present measurement we obtained $\delta=0.55\pm0.10$ mm/sec.

IV.5. Normal α-Fe_2O_3 (>1000Å)

As this absorber is antiferromagnetic and has rather lower symmetrical crystal structure, the mixed interaction of magnetic dipole and electric quadrupole would be expected.

It is well known[13,14] that α-Fe_2O_3 exhibits a weak parasitic ferromagnetism above the Morin temperature (~260°K), where the electron spins align perpendicular to the 3-fold axis of rhombohedral structure (c-axis), due to the slightly canted spins nearly in the basal plane (c-plane), while the ferromagnetism disappears below the temperature, where the spins align parallel to the c-axis. This spin flopping is called the Morin transition. Since the principal axis of the nuclear quadrupole moment Q aligns parallel to the internal magnetic field H_i and the electric field gradient ∇E is parallel to the c-axis due to the uni-axial symmetry, θ in Eq. (12) is 0° above ~260°K and 90° below this temperature. Then,

$$\left.\begin{aligned}&\varepsilon(\pm3/2)=-e^2qQ/8,\quad \varepsilon(\pm1/2)=e^2qQ/8 \quad \text{at room temperature,}\\ &\varepsilon(\pm3/2)=e^2qQ/4,\quad \varepsilon(\pm1/2)=-e^2qQ/4 \quad \text{at low temperature.}\end{aligned}\right\} \tag{13}$$

The difference between $S_{1,2}$ and $S_{5,6}$ can be given by

$$\left.\begin{aligned}&S_{1,2}-S_{5,6}=4\varepsilon=e^2qQ/2 \quad \text{at room temperature,}\\ &S_{1,2}-S_{5,6}=4\varepsilon=-e^2qQ \quad \text{at low temperature.}\end{aligned}\right\} \tag{14}$$

Ono and Ito[15] have recently measured the Mössbauer absorption of α-Fe_2O_3 at various temperatures and found the ratio of ε at 100°K and at 300°K being about $-2:1$. This result is in agreement with that given by Eq. (14). They thus confirmed that a hypothesis of the spin flopping at the Morin temperature

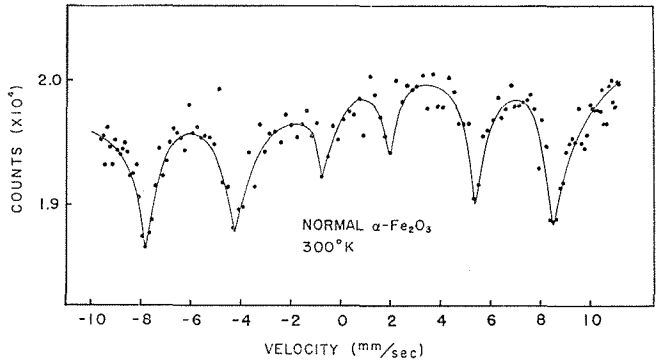

Fig. 11. Mössbauer absorption spectrum in a normal α-Fe_2O_3 (>1000Å) absorber at 300°K.

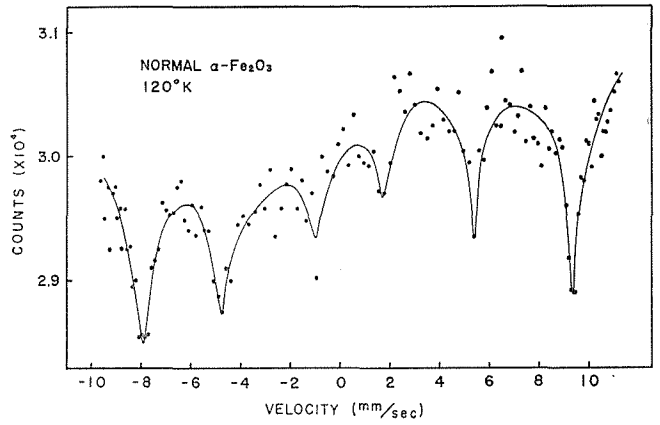

Fig. 12. Mössbauer absorption spectrum in a normal α-Fe_2O_3 (>1000Å) absorber at 120°K.

is valid. From our measurements at room temperature (300°K) and at low temperature (120°K), as shown in Figs. 11 and 12, we could obtain as

$$S_{1,2}-S_{5,6}=-0.85\pm0.05 \text{ mm/sec} \quad \text{at } 120°\text{K},$$
$$S_{1,2}-S_{5,6}=0.40\pm0.05 \text{ mm/sec} \quad \text{at } 300°\text{K}.$$

Hence $$\varepsilon(\text{at } 120°\text{K})/\varepsilon(\text{at } 300°\text{K})=-2.1\pm0.3.$$

This result also agrees with that derived from Eq. (14) within a limit of experimental errors.

The internal magnetic field in α-Fe_2O_3 was obtained, by applying Eq. (11) and adopting $H_i(\text{Fe})=333$ kOe, as

$$H_i=542\pm15 \text{ kOe} \quad \text{at } 120°\text{K},$$
$$H_i=515\pm15 \text{ kOe} \quad \text{at } 300°\text{K}.$$

This value of H_i at 300°K is quite similar to that found by Kistner and Sunyar[16]. The results found by the present measurement are also, within accuracies of experimental errors, in good agreement with the temperature dependence expected from the Brillouin function for $S=5/2$.

The isomer shifts were also found as

$$\delta = 0.52 \pm 0.05 \text{ mm/sec} \quad \text{at } 120°\text{K},$$
$$\delta = 0.45 \pm 0.05 \text{ mm/sec} \quad \text{at } 300°\text{K}.$$

The value of 0.45 mm/sec at room temperature well agrees with that of 0.47 mm/sec reported by Walker *et al.*[17]. The temperature shift of 0.07 mm/sec between at 120°K and at 300°K is about a half compared with a value of $(3R/2Mc^2)E_0 \cdot \Delta T = 0.13$ mm/sec, which corresponds to the second order Doppler shift calculated by Pound and Rebka[18], where E_0 is the 14.4-keV gamma-ray energy, R is the gas constant and M is the gram atomic weight of iron.

IV.6. Ultra-fine Particles of α-Fe_2O_3

For an absorber of ultra-fine particles of α-Fe_2O_3 we have dealt with two problems; one is the Morin transition and internal magnetic field in α-Fe_2O_3 itself and the other is Mössbauer effect of ultra-fine particles[19].

The samples used was prepared by the method described in Sec. III.2. The particle size was estimated by observing the broadening of X-ray diffraction peaks.

When the size of the ferromagnetic or antiferromagnetic particle is very small, less than about 100Å, the anisotropy energy KV decreases to be comparable with kT, where V is the volume of the particle and K is the anisotropy energy per unit volume. In this case, the particle magnetization vector becomes unstable by thermal agitation, and it shows the paramagnetic behavior as having a large magnetic moment. Such a thermal equilibrium behavior has been named "superparamagnetism"[20,21]. In the paramagnetic state of an-

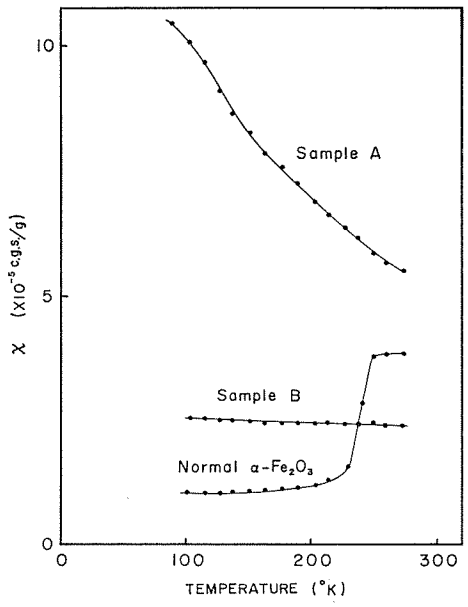

Fig. 13. Variation with temperature of the antiferromagnetic susceptibility of α-Fe_2O_3. The particle sizes of the samples A and B are about 50Å and 150Å, respectively, while that of the normal sample is >1000Å.

tiferromagnetic particles as α-Fe_2O_3, each particle has magnetic moments and the magnetic susceptibility increases[22~24].

The susceptibility of the samples used was measured as a function of temperature, as shown in Fig. 13. The particle sizes of samples A and B are about 50Å and 150Å, respectively. Figures 14~17 show the Mössbauer absorption spectra obtained with samples A and B at 120°K and 300°K.

The spectrum shown in Fig. 14 exhibits two different features from that obtained with normal α-Fe_2O_3 at 120°K. One is that the sign of the quadrupole interaction, ε, derived from $S_{1,2}-S_{5,6}$ for the sample A is reversed and a value of ε is approximately a half of that for normal α-Fe_2O_3 at 120°K. While, as is seen in Fig. 14, the spectrum at 120°K gives a value of ε nearly equal to that for normal α-Fe_2O_3 at room temperature, 300°K. In regard to ε, as can be understood from Figs. 16 and 17, the spectra with the sample B at 120°K and 300°K show similar feature to that with the sample A at 120°K. From this

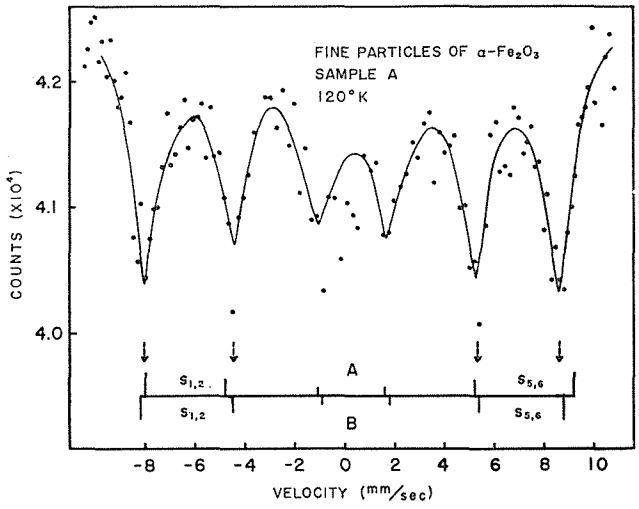

Fig. 14. Mössbauer absorption spectrum in sample A of α-Fe_2O_3 (~50Å) at 120°K. A and B show the peak positions of normal α-Fe_2O_3 at 120°K and 300°K, respectively. $S_{1,2}$ and $S_{5,6}$ show the separations between line 1 and 2, and 5 and 6, respectively.

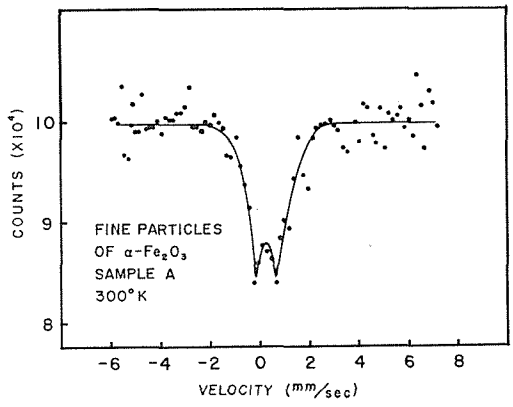

Fig. 15. Mössbauer absorption spectrum in sample A of α-Fe_2O_3 (~50Å) at 300°K.

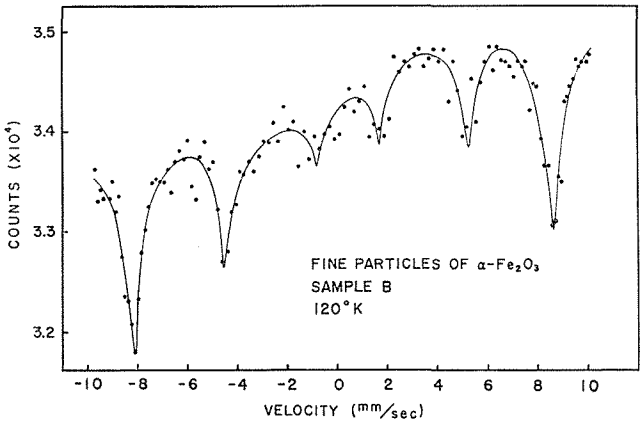

Fig. 16. Mössbauer absorption spectrum in sample B of α-Fe_2O_3 (~150Å) at 120°K.

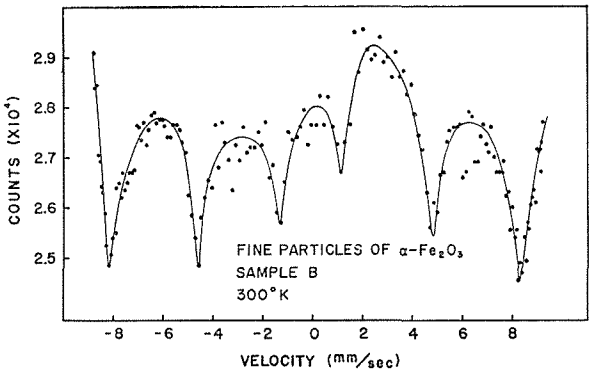

Fig. 17. Mössbauer absorption spectrum in sample B of α-Fe_2O_3 (~150Å) at 300°K.

experimental finding it can be concluded that the ultra-fine particles examined have no Morin transition above at least 120°K and electron spins lie still in the basal plane (c-plane).

The other evidence found is that the internal magnetic fields in samples A and B are both slightly smaller than that in the normal size particle. The result obtained is given in Table 1.

This fact suggests that the molecular field acting on each spin decreases in the ultra-fine particles of α-Fe_2O_3. However, further study should be necessary to get accurate information on the dependence of H_i on the particle size.

Table 1. Internal magnetic fields in α-Fe_2O_3 samples.

Sample	at 120°K (kOe)	at 300°K (kOe)
Sample A (~50Å)	529±15	0
Sample B (~150Å)	531±15	497±15
Normal size (>1000Å)	542±15	515±15

The spectrum of the sample A at 300°K shows only two lines by the quadrupole interaction, as shown in Fig. 15. This phenomenon may be explained by a motional narrowing due to the rapid relaxation of antiferromagnetic spins compared with the nuclear Larmor precession. In the ultra-fine particles the antiferromagnetic spins are fluctuated by themal agitation and its relaxation time becomes smaller than the reciprocal of the nuclear Larmor frequency (10^{-8} sec). By this reason, in this case Fe nucleus is not suffering from the internal magnetic field and the Zeeman splitting is not observed.

The transition temperature from the six-line- to two-line-spectrum may lie between 120°K and 300°K for most of particles in the sample A. The observed spread of experimental points in the middle region of the spectrum, as shown in Fig. 14, may be caused by a small fraction of the sample particles having a rapid relaxation even at 120°K. While, as for the sample B, both spectra at 120°K and 300°K have six peaks, as shown in Figs. 16 and 17. It can be, therefore, asserted that a critical particle size for this transition should be between ~50Å and ~150Å at 300°K.

The relaxation time of the magnetization vector in a single-domain particle has been given by Néel[25] as

$$\frac{1}{\tau}=\frac{1}{f_0}\exp(-KV/kT), \quad f_0\simeq 10^9\ \mathrm{sec}^{-1}. \tag{15}$$

To estimate it, the value of the potential barrier, KV, originated from the magnetic anisotropy is necessary to know. In the present case, as the antiferromagnetic spins rotate in the basal plane preferentially, one has to treat an anisotropy energy in the plane as a potential barrier. The quantitative discussion on this point is impossible, since a value of the anisotropy constant, K, in the plane has not yet been given definitely[26] and the volume of the particles in the sample used can not also be determined by lack of knowing the shape of the particles.

It is interesting to note that for a critical relaxation time, τ_c, corresponding to this transition there would exist a critical temperature for a given particle size or a critical particle size for a given temperature, as can be understood from Eq. (15), where τ_c is believed to be comparable with the reciprocal of the Lamor frequency, ~10^{-8} sec. The experiment to obtain a quantitative relation between these values may, therefore, provide an information on a value of K.

An experiment with the sample A was carried out at some temperatures between 120°K and 300°K. It is noted that in the absorption spectrum taken at 210°K experimental points were scattered so irregularly that any line could not be discriminated. In order to get any definite information on the problem of interest further experimental study with more elaborated apparatus and technique should be desired.

As described in Chap. II, the theoretical derivation of the recoilless fraction is basing upon an assumption that when a nucleus embedded in a solid emits or absorbs a gamma-ray photon, a fraction of the nuclear transition energy concerned going into motion of the entire solid is extremely small and

will be neglected. However, it may be supposed that when the particles of the absorber or emitter are very minute this assumption would be invalid and the recoilless fraction would be affected by the particle size. From our observations of the absorption spectra at 120°K we attempted to measure the ratio of the recoilless fractions and obtained a rough value as normal sample (>1000Å) : sample B(~150Å) : sample A(~50Å) = 1.0 : 0.96 : 0.52. However, as this value is very rough one, it can serve only as an index for the problem of our interests. More accurate and careful measurements with the particles of various sizes should be necessary.

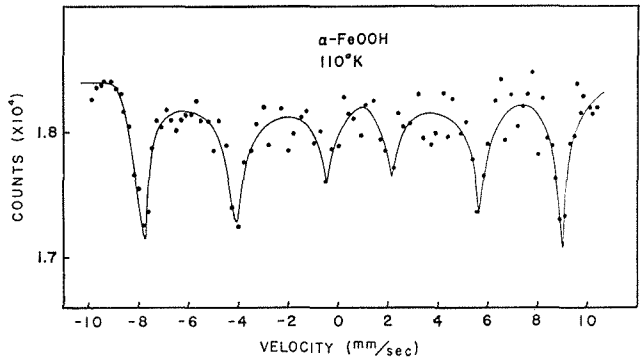

Fig. 18. Mössbauer absorption spectrum in α-FeOOH at 110°K.

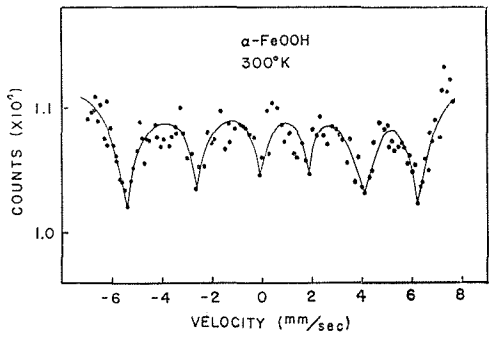

Fig. 19. Mössbauer absorption spectrum in α-FeOOH at 300°K.

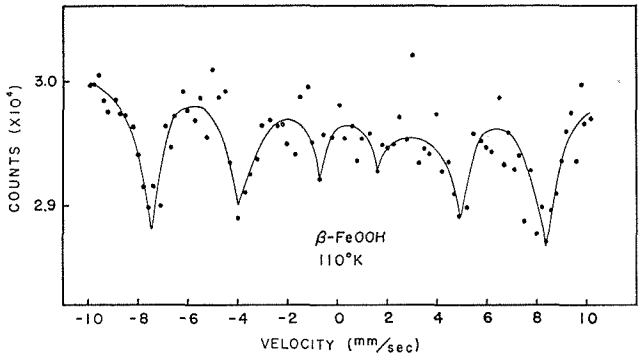

Fig. 20. Mössbauer absorption spectrum in β-FeOOH at 110°K.

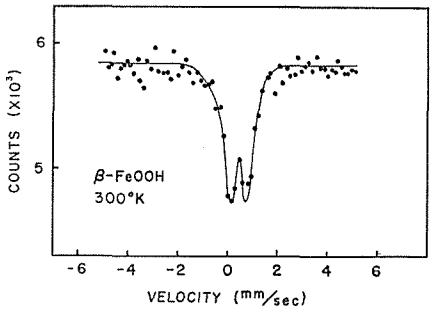

Fig. 21. Mössbaurer absorption spectrum in β-FeOOH at 300°K.

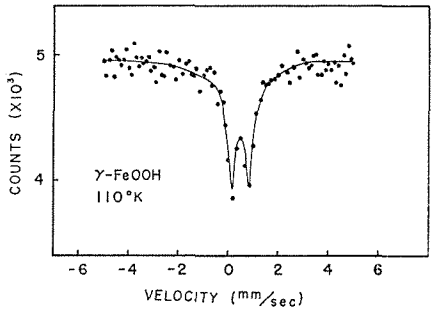

Fig. 22. Mössbauer absorption spectrum in γ-FeOOH at 110°K.

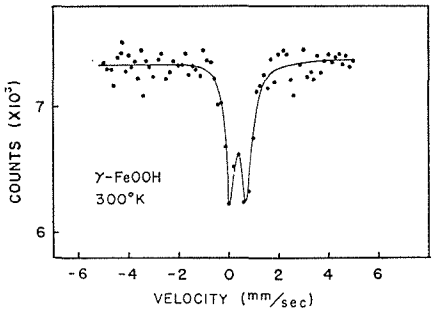

Fig. 23. Mössbauer absorption spectrum in γ-FeOOH at 300°K.

The interesting problems on the dependence of isomer shift, internal magnetic field and quadrupole interaction upon the particle size are left to be studied experimentally in the future.

IV.7. α-FeOOH, β-FeOOH and γ-FeOOH

The crystal structures of these isomers of iron oxyhydrates have recently been disclosed[27,28], however, their magnetic properties, especially whether to be antiferromagnetic or not, have not yet been established. By means of observing the Mössbauer absorption spectra we attempted to clarify some obscure points with these isomers[29].

The results of our measurements are shown in Figs. 18~23. The experimental values of internal magnetic field, H_i, and isomer shift, δ, obtained are

Table 2. Internal magnetic field, H_i, and isomer shift, δ, of α-, β- and γ-FeOOH.

Sample		H_i(kOe)	δ(mm/sec)
α-FeOOH	(110°K)	520±15	0.7 ±0.1
	(300°K)	360±15	0.55±0.1
β-FeOOH	(110°K)	490±15	0.45±0.1
	(300°K)	0	0.45±0.1
γ-FeOOH	(110°K)	0	0.5 ±0.1
	(300°K)	0	0.4 ±0.1

listed in Table 2.

The absorption spectra of α-FeOOH at both 110°K and 300°K, as shown in Figs. 18 and 19, showed the six-line splitting due to the antiferromagnetic electron spin ordering. It has been shown empirically by Walker *et al.*[17] that the Mössbauer effect of tri-valent iron ($3d^5$) in ionic compounds has an internal magnetic field of 500~550 kOe at 0°K and an isomer shift of 0.5 mm/sec. By the present work the values of the internal field and isomer shift in α-FeOOH were found to be close to the typical values of these in $3d^5$ electronic configuration. If the temperature dependence of the internal field corresponds to the Brillouin function for $S=5/2$, the Néel temperature can be derived to be in the vicinity of 400°K.

The spectrum of β-FeOOH showed the six-line splitting at 110°K while only a doublet due to the quadrupole effect at 300°K, as shown in Figs. 20 and 21. The Néel temperature of it, therefore, should lie between 110°K and 300°K.

No line splitting by the internal field was observed in the absorption spectra of γ-FeOOH at both 110°K and 300°K. From this fact, this compound is believed to be paramagnetic down to 110°K.

It is also noted that the isomer shifts in β- and γ-FeOOH are both close to the typical value for $3d^5$ configuration, as given in Table 2.

V. SUMMARY

The Mössbauer absorption spectra of several iron compounds have been observed using ^{57}Fe as a source. Metallic iron and stainless steel were used as calibrations for the estimation of the source velocity.

The quadrupole effect and isomer shift have been measured with $FeSO_4 \cdot 7H_2O$ which is a paramagnetic salt. From the absorption spectra of Fe_2B of ferromagnetic nature an intensity of the internal magnetic field has been measured. By the observation with normal α-Fe_2O_3 (>1000Å) it has been confirmed that a hypothesis of spin flopping at the Morin temperature is valid.

As a result of the observations with the ultra-fine α-Fe_2O_3 particles with sizes of about 50Å and 150Å it has been found that the ultra-fine particles such as those used in the present work have no Morin transition above at least 120°K. The spectrum of the particles of 50Å taken at 120°K showed six-line splitting, while at 300°K showed only two lines. This phenomenon may be explained by a motional narrowing due to the rapid relaxation of antiferromagnetic spins compared with the nuclear Larmor precession (~10^{-8} sec). The critical volume of particles and critical temperature for this transition have been found to be between 50Å and 150Å at 300°K and between 120°K and 300°K for particles of 50Å, respectively. It has also been found that for the ultra-fine particles the recoilless fraction would decrease from that obtained with larger particles.

From the measurements of the Mössbauer absorption with α-, β- and γ-FeOOH some magnetic properties of these isomers of iron oxyhydrate have been disclosed as follows: the Néel temperature for α-FeOOH may be close to

400°K and that for β-FeOOH may lie between 110°K and 300°K, while γ-FeOOH is paramagnetic above at least 110°K.

ACKNOWLEDGMENTS

The unsparing cooperation of T. Shinjo, Y. Endoh and M. Shiga during the whole course of the present work are much appreciated. It is a pleasure to thank Professor T. Takada and Dr. Y. Bando and N. Yamamoto for their kind providing of all iron compounds used. We are indebted to R. Katano for his help in constructing the electronic circuits. The authors are also particularly grateful to these colleagues and to Professor Y. Nakamura for their suggesting the possible interpretation of the experimental data and for many stimulating discussions throughout the course of the work.

REFERENCES

(1) R. L. Mössbauer, *Z. Physik*, **151**, 124 (1958).
(2) J. Frenkel and J. Dorfman, *Nature*, **126**, 274 (1930).
(3) M. L. Néel, *Compt. rend.*, **224**, 1448 (1947); *Appl. Sci. Research*, **B4**, 13 (1954).
(4) H. J. Lipkin, *Ann. Phys.*, **9**, 332 (1960).
(5) W. M. Visscher, Unpublished note (1961). See Ref. (6), p. 45.
(6) H. Frauenfelder, "The Mössbauer Effect", W. A. Benjamin, Inc., New York, 1962, p. 53.
(7) A. Abragam, "The Principles of Nuclear Magnetism", The Clarendon Press, Oxford, 1961.
(8) A. J. E. Boyle and H. E. Hall, *Rep. Progr. Phys.*, **25**, 441 (1962).
(9) W. Kerler, W. Neuwirth, E. Fluck, P. Kuhn and B. Zimmermann, *Z. Physik*, **173**, 321 (1963).
(10) S. S. Hanna, J. Heberle, C. Littlejohn, G. J. Perlow, R. S. Preston and D. H. Vincent, *Phys. Rev. Letters*, **4**, 28 (1960); **4**, 177 (1960).
(11) R. S. Preston, S. S. Hanna and J. Heberle, *Phys. Rev.*, **128**, 2207 (1962).
(12) S. DeBenedetti, G. Lang and R. Ingalls, *Phys. Rev. Letters*, **6**, 60 (1961).
(13) M. L. Néel, *Rev. Mod. Phys.*, **25**, 58 (1953).
(14) S. T. Lin, *Phys. Rev.*, **116**, 1447 (1959); *J. Appl. Phys.*, **31**, Suppl., 273S (1960).
(15) K. Ono and A. Ito, *J. Phys. Soc., Japan*, **17**, 1012 (1962).
(16) O. C. Kistner and A. W. Sunyar, *Phys. Rev. Letters*, **4**, 412 (1960).
(17) L. R. Walker, G. K. Wertheim and V. Jaccarino, *Phys. Rev. Letters*, **6**, 98 (1961).
(18) R. V. Pound and G. A. Rebka, Jr., *Phys. Rev. Letters*, **4**, 274 (1960).
(19) T. Nakamura, T. Shinjo, Y. Endoh, N. Yamamoto, M. Shiga and Y. Nakamura, *Phys. Letters*, to be published.
(20) C. P. Bean, *J. Appl. Phys.*, **26**, 1381 (1955).
(21) C. P. Bean and J. D. Livingston, *J. Appl. Phys.*, **30**, Suppl., 120S (1959).
(22) J. Cohen, K. M. Creer, R. Pauthenet and K. Strivastava, *J. Phys. Soc., Japan*, **17**, Suppl., B-1, 685 (1962).
(23) K. M. Creer, *J. Phys. Soc., Japan*, **17**, Suppl., B-1, 690 (1962).
(24) T. Takada and N. Kawai, *J. Phys. Soc., Japan*, **17**, Suppl., B-1, 691 (1962).
(25) M. L. Néel, *Ann. Geophys.*, **5**, 99 (1949).
(26) P. J. Flanders and W. J. Schuele, *Phil, Mag.*, **9**, 485 (1964).
(27) G. L. Peacock, *Trans. Roy. Soc. Can.*, **36IV**, 116 (1942).
(28) A. L. Mackay, *Mineral. Mag.*, **32**, 545 (1960).
(29) T. Takada, M. Kiyama, Y. Bando, T. Nakamura, M. Shiga, T. Shinjo, N. Yamamoto, Y. Endoh and H. Takaki, *J. Phys. Soc., Japan*, **19**, 1744 (1964).